STUDY ON PERFORMANCE OF ULTRA-HIGH PRESSURE VESSEL OF WATER TOWER UNDER UNSTEADY ENVIRONMENT WITH PFEM

Hui SONG[1*], Guozhi ZHANG[2]

The working environment of the high-pressure vessel of the water tower is poor and random. The impact of randomness in geometric parameters, material parameters and loading parameters on the reliability of the ultra-high pressure vessels in water towers is studied. Based on the improvement in the design of the overall structure, the theoretical model of the variance of the maximum stress is established. Based on the theoretical reliability model, the reliability is calculated as 1 to determine the working reliability. Moreover, the PFEM (perturbation finite element method) combined with response surface statistical analysis method to analyze the randomness of geometric parameters, material parameters and loading parameters. The analysis results show that the maximum equivalent stress is 268.05 MPa, and 95% of the maximum equivalent stress of the overall structure is less than 210 MPa. There is no stress concentration at the joint and it is reliable. The results provide an analytical method and theory foundation for the design of the high pressure vessel in water towers.

Keywords: ultra-high pressure vessel; geometric parameters; material parameters; loading parameters; reliability; PFEM

1. Introduction

Lightweight design and reliability analysis of the manufacturing industry have always been a hot spot. The manufacturing level of special large pressure vessels is an important reflection of a strong manufacturing country. As pressure vessels are important equipment in industries such as petroleum, chemical, energy, aerospace, and construction, strict requirements are placed on their quality, safety, and reliability [1-3]. Therefore, the lightweight design and reliability analysis of pressure vessels should be approached with even greater caution. Lightweight is the optimization goal of large equipment, but if it is too lightweight, it may result in insufficient reliability in operation. Strictly, there is a certain "contradiction" between them. At the same time, due to the harsh working conditions such as

[1] Architecture School, Xinxiang Vocational and Technical College, Xinxiang, 453000, China

[2] Mechanical and Electrical Engineering School, Xinxiang University, Xinxiang, 453000, China

[*] Corresponding author: Email: 869763442@qq.com

loading, its reliability is particularly important. Redundant design for transitional safety can also cause material waste and improve its long-term overloaded work.

Large pressure vessels have always been a focus in engineering. For a long time, people have explored the design, manufacturing, and effective process measures of special large pressure vessels combined with theory, simulation and practice [4-5]. Many results have been achieved in structural design [6-7], crack propagation [8-9], and stress detection [10-11] of pressure vessels. In structural design of pressure vessels, a safe and efficient composite outer packaging pressure vessel (COPV) for hydrogen storage is studied, including layer thickness, stacking sequence, and the development of a particularly robust design model for the dome area. The predictive behavior and failure model are developed, and an accurate software program considering multiple factors of the fiber winding process is developed [12]. In the crack propagation mechanism of pressure vessels, the strain energy release rate is derived from the relationship between the stress intensity factor and the effective elastic modulus of the composite material storage tank. The exported stress intensity factor shows that the fracture resistance of specific composite shell and lining materials is significantly improved, particularly in higher winding directions. The results emphasize the superior performance of boron epoxy composite shell for type III pressure vessels, showing the lowest stress intensity factor value and excellent crack resistance. In contract, the glass epoxy resin shell is more sensitive to crack propagation, especially in specific layer orientations [13]. In stress detection and monitoring of pressure vessels, the reactor pressure vessel is located at the center of the nuclear containment building, including nuclear fuel. There is a risk of radiation leakage in the nuclear power plant when there is an earthquake. It is crucial to determine the stress intensity for evaluating structural integrity and analyzing the seismic response of the reactor pressure vessel to prevent serious disasters. A stress intensity regression model using signal extraction methods and machine learning is proposed. It combines the finite element model to enable us to immediately predict the stress intensity only based on signal features and properties. This may be an additional verification tool to ensure safety of nuclear power plants [14]. In addition, with the sudden changes in the world environment, the construction and maintenance of emergency facilities have become increasingly important, especially during floods. Water towers are important building facilities for regulating and storing water, and pressure vessels are an important component of water towers. In recent years, research on water tower pressure vessels [15-16] has also become a hot spot. The reliability for large pressure vessels in water towers is even more prominent, because its destruction may cause huge disasters.

Health monitoring of large special equipment is also important. The reliability analysis on the operational performance of special water tower ultra-high pressure vessels is not yet in-depth and systematic. To ensure reliable and

safe operation of pressure vessels in water towers, the high-pressure vessel of the water tower under high humidity and heat environment is still needed to be studied. To this end, a theoretical mechanical model of the reliability of the water tower pressure vessel is established based on elastic mechanics and probability theory. Based on PFEM, the randomness of material parameters (elastic modulus and Poisson ratio), geometric parameters (diameter and thickness), and load parameters (internal pressure) are taken in to account. The influence of its reliability is deeply and systematically studied.

2. Establishment and analysis of limit theoretical model

2.1 Establishment of weighted coordination and combination limit theoretical model

Based on the axial symmetry solution of elastic mechanics, the ultra-high pressure vessel is divided into the cylindrical part and the spherical part. Considering the comprehensive coordination of the two parts, a more accurate theoretical model is derived based on the weighted coordination idea.

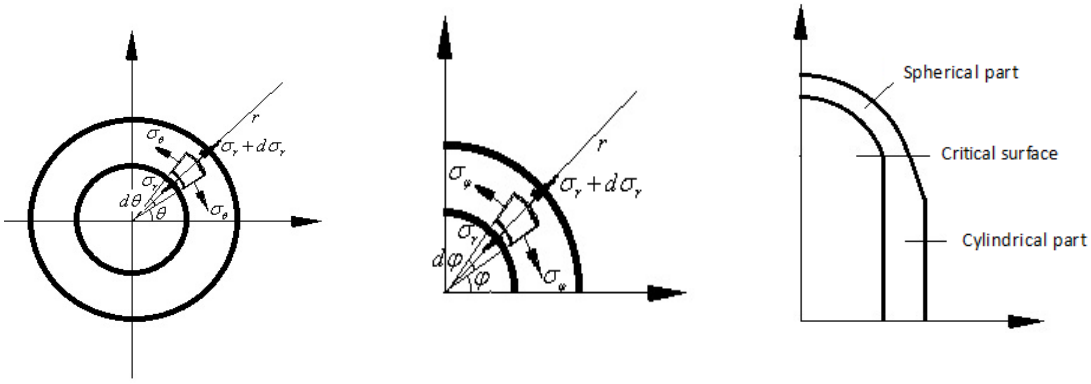

(a) The cylindrical part (b) The spherical part (c) Combined shape

Fig. 1 Stress analysis diagram of pressure vessel

2.1.1 Theoretical model of cylindrical part

The stress diagram of the cylindrical part is shown in Fig. 1(a). Because the force of the micro-plasma is balanced along the radial direction

$$\sum F_{ri} = 0 \tag{1}$$

There is

$$(\sigma_r + d\sigma_r)(r + dr)dz - \sigma_r r d\theta dz - 2\sigma_\theta dr \sin\frac{d\theta}{2} dz = 0 \tag{2}$$

where, σ_r is the radial stress, and σ_θ is the circumferential stress.

When $d\theta \to 0$

$$\sin\frac{d\theta}{2} \to \frac{d\theta}{2} \tag{3}$$

Skip the high order infinitesimal and sort out

$$2\sigma_r + r\frac{d\sigma_r}{dr} = \sigma_r + \sigma_\theta \tag{4}$$

Because it is plane simplification of axial symmetry problem

$$\sigma_r + \sigma_\theta = 2C \tag{5}$$

Substitute Eq. (5) into Eq. (4), after integral, there is

$$\begin{cases} \sigma_r = C + \dfrac{D}{r^2} \\ \sigma_\theta = C - \dfrac{D}{r^2} \end{cases} \tag{6}$$

Boundary condition is

$$\begin{cases} \sigma_r = -p & r = r_1 \\ \sigma_r = 0 & r = r_1 + t_1 \end{cases} \tag{7}$$

where, p is the internal pressure; r_1 is the inner radius of cylindrical part, and t_1 is the wall thickness.

Therefore, the radial stress and circumferential stress are as follows:

$$\begin{cases} \sigma_r = -\dfrac{r_1^2 p}{t_1(2r_1 + t_1)}\left[\left(\dfrac{r_1 + t_1}{r}\right)^2 - 1\right] \\ \sigma_\theta = \dfrac{r_1^2 p}{t_1(2r_1 + t_1)}\left[\left(\dfrac{r_1 + t_1}{r}\right)^2 + 1\right] \end{cases} \tag{8}$$

Based on Eq. (8), the circumferential stress at the inner diameter and outer diameter of the cylinder is as follows:

$$\begin{cases} \sigma_\theta\big|_{r=r_1} = \dfrac{2r_1^2 + t_1^2 + 2r_1 t_1}{t_1(2r_1 + t_1)} p \\ \sigma_\theta\big|_{r=r_1+t_1} = \dfrac{2r_1^2}{t_1(2r_1 + t_1)} p \end{cases} \tag{9}$$

When the thickness of the cylinder is small relative to the inner diameter of the cylinder, there is

$$\sigma_\theta = \lim_{t_1 \to 0} \sigma_\theta\big|_{r=r_1} = \lim_{t_1 \to 0} \frac{2r_1^2 + t_1^2 + 2r_1 t_1}{t_1(2r_1 + t_1)} p = \lim_{t_1 \to 0} \sigma_\theta\big|_{r=r_1} = \lim_{t_1 \to 0} \frac{2r_1^2}{t_1(2r_1 + t_1)} p = \frac{r_1}{t_1} p \tag{10}$$

2.1.2 Theoretical model of spherical part

The stress diagram of the spherical part is shown in Fig. 1(b). Because the force of the spherical crown micro-plasma is balanced along the radial direction

$$\sum F_{ri} = 0 \tag{11}$$

There is

$$(\sigma_r + d\sigma_r)2\pi(r+dr)^2[\sin(\varphi+d\varphi)-\sin\varphi]-\sigma_r 2\pi r^2[\sin(\varphi+d\varphi)-\sin\varphi]-2\sigma_\varphi 2\pi r dr\sin\frac{d\varphi}{2}=0 \tag{12}$$

Skip the high order infinitesimal and sort out

$$2(\sigma_r\cos\varphi-\sigma_\varphi)+r\cos\varphi\frac{d\sigma_r}{dr}=0 \tag{13}$$

Due to $\cos\theta \le 1$, there is

$$2(\sigma_r-\sigma_\varphi)+r\frac{d\sigma_r}{dr}\ge 0 \tag{14}$$

Compared with the solution results of the cylindrical part, the limit circumferential stress and the limit latitudinal stress of the spherical part are as follows:

$$\sigma_\theta=\sigma_\varphi\approx\frac{r_0}{2t_0}p \tag{15}$$

where, r_0 is the inner radius of spherical part, and t_0 is the wall thickness.

Comparing Eq. (14) with Eq. (15), regardless of whether it is spherical or cylindrical, the latitudinal stress is proportional to the radius and internal pressure, and inversely proportional to the thickness. Under the same radius, thickness and internal pressure, the latitudinal stress of a spherical shape is about half of a cylindrical shape. Under the same load and geometric parameters, this means that the stress of a spherical shape is smaller than that of a cylindrical shape, which means that the load-bearing capacity of a spherical shape is greater. In engineering practice, the thickness of the cylindrical part is thick and the thickness of the spherical part is thinner, which means that the existence of a transition section is reasonable. Of course, comparing with the cylindrical part, the storage volume of the spherical part has been significantly reduced.

2.1.3 Weighted coordination theoretical model

According to Fig.1(c), the ultra-high pressure vessel shall be mechanically coordinated at the junction of spherical and cylindrical shape. Considering the boundary coordination conditions and combined Eq. (10) with Eq. (15), there is

$$\frac{r_0}{2t_0}p\cdot 2\pi r_1 t_0\cdot a=\frac{r_1}{t_1}p\cdot 2\pi r_1 t_0\cdot b \tag{16}$$

where, a and b are the adjustment coefficients.

So

$$a = 2\frac{r_1 t_0}{r_0 t_1} b \tag{17}$$

Based on the idea of weight weighting, and considering boundary coordination conditions, there is

$$\sigma_\theta = \frac{r_0}{2t_0} p \cdot \frac{a}{a+b} + \frac{r_1}{t_1} p \cdot \frac{b}{a+b} \tag{18}$$

Further, the circumferential stress of the spherical part of the ultra-high pressure vessel is as follows:

$$\sigma_\theta = \frac{2r_0 r_1}{2r_1 t_0 + r_0 t_1} p = \frac{pr_0}{\left(1 + \frac{r_0 t_1}{2r_1 t_0}\right) t_0} = \frac{pr_0}{(1+\varpi_0) t_0} \tag{19}$$

where, ϖ_0 is the shape influence coefficient, and expressed as follows:

$$\varpi_0 = \frac{r_0 t_1}{2r_1 t_0} \tag{20}$$

2.1.4 Error analysis of theoretical model established

When the parameters of the ultra-high pressure vessel of the water tower are: $r_0 = 2500\,\text{mm}$, $r_1 = 2200\,\text{mm}$, $t_0 = 150\,\text{mm}$, $t_1 = 310\,\text{mm}$, $p = 20\text{MPa}$. According to Eq. (20), the shape influence coefficient of the ultrahigh pressure vessel is calculated as follows: $\varpi_0 = 1.174$ (21)

Based on Burger equation, the maximum stress $\sigma_{\max}$ is as follows:

$$\sigma_{\max} = \sigma_\theta = \sigma_\varphi = \frac{pr_0}{2t_0} \tag{22}$$

Based on Eq. (19), the maximum stress $\sigma_{\max}$ is as follows:

$$\sigma_{\max} = \sigma_\theta = \sigma_\varphi = \frac{pr_0}{(1+\varpi_0) t_0} \tag{23}$$

According to Eq. (22), the maximum circumferential stress of the ultra-high pressure vessel calculated is 167MPa. According to Eq. (23), the maximum circumferential stress of the ultra-high pressure vessel is 153MPa. The maximum circumferential stress calculated by the finite element method is 155MPa. Compared with the calculation results of the finite element method, the calculation error based on Burger equation is 7.8%, and that based on the weighted coordination theoretical model is 1.3%. The weighted coordination theoretical model is more accurate. This also indicates that the element density of the finite element model is reasonable.

2.2 Theoretical model of maximum stress variance

Based on the probability theory and Eq. (23), the standard deviation of the maximum stress $\delta_{s\max}$ is expressed as follows:

$$\delta_{s\max} = \frac{1}{(1+\varpi_0)t_0}\sqrt{r^2\delta_p{}^2 + p^2\delta_r{}^2 + \frac{p^2 r_0{}^2}{t_0{}^2}\delta_t{}^2} \tag{24}$$

where, δ_p, δ_r and δ_t are the standard deviation of internal pressure, inner radius, and wall thickness, respectively.

Based on the calculation model of reliability of structures, the reliability is expressed as follows:

$$R = 1 - \Phi\left[\frac{\sigma_{\max} - \sigma_{str}}{\sqrt{\delta_{sstr}^2 + \delta_{s\max}^2}}\right] \tag{25}$$

where, σ_{str} is the allowable stress, and the standard deviation of allowable stress δ_{sstr} is $0.11\,\sigma_{str}$ depending on practical experience.

When the parameters of the ultrahigh pressure vessel of a water tower are $\delta_r = 10$ mm, $t_0 = 150$ mm, $\delta_t = 6$ mm, $\delta_p = 2.5$ Mpa, $\sigma_{str} = 420$ Mpa, and $\delta_{sstr} = 46.2$ MPa, based on Eq. (24), the standard deviation of the maximum stress is $\delta_{s\max} = 23.12$ MPa. The reliability is 1 based on Eq. (25).

3. Analysis of ultra-high pressure vessel with perturbation finite element method

3.1 Establishment of the finite element model

Before the finite element model is established, the length of the cylindrical part should be determined and calculated as follows:

$$L = 2.5\sqrt{r_0 t_1} \tag{26}$$

where, t_1 is the thickness of the cylindrical part.

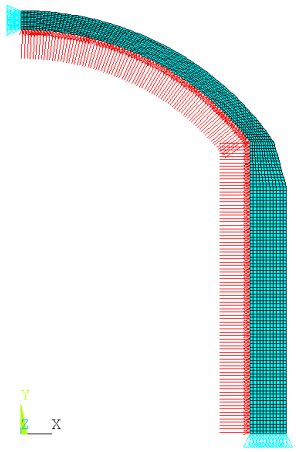

Fig. 2 Finite element model

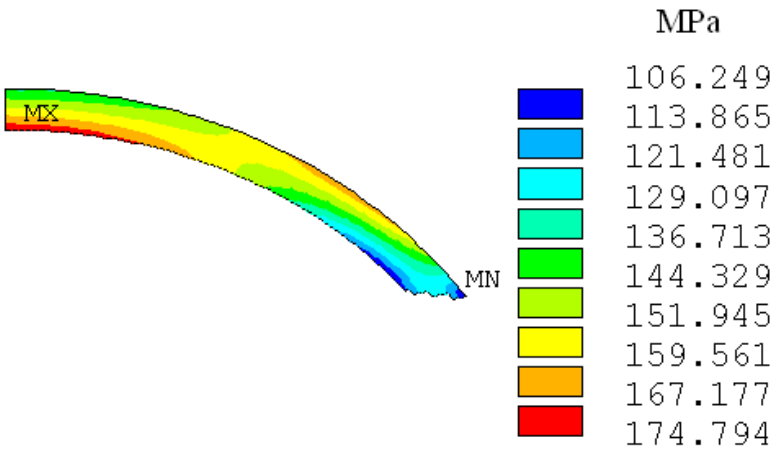

Fig. 3 Equivalent stress distribution

Based on the analysis of the bearing and storage capacity of the cylindrical and spherical parts, Eq. (26) should be used for engineering design to make the stress of the cylindrical and spherical parts be more balanced. During the coordination transition phase, the occurrence of stress concentration should be minimized as much as possible. Finite element analysis also proves this point.

The thickness of the cylindrical part is 310mm. Based on Eq. (26), the length of the cylindrical part is 2163.3mm, and 2200mm is taken. Other parameters are the same as the above theoretical analysis. Due to the axial symmetry of structure, loads and constraint conditions, a finite element model is established, as shown in Fig. 2. The finite element results are shown in Fig. 3. From Fig. 3, it can be seen that the maximum equivalent stress is located inside its top, at 174.794 Mpa.

3.2 Analysis of the influence of the randomness of parameters on the performance

Further reliability analysis is conducted based on perturbation finite element method. In calculation, the application of parameterization technology can ensure the consistency of element density, and the size variation range of the pressure vessel is not large, thereby ensuring the accuracy of the calculation. Its parameters and corresponding symbols in reliability analysis are shown in Table 1, and these parameters are attached to Gauss distribution. The central composite sampling method and Monte Carlo extending sampling method are used. The number of iterations for central composite sampling is 27, and that for Monte Carlo extended sampling is 10000.

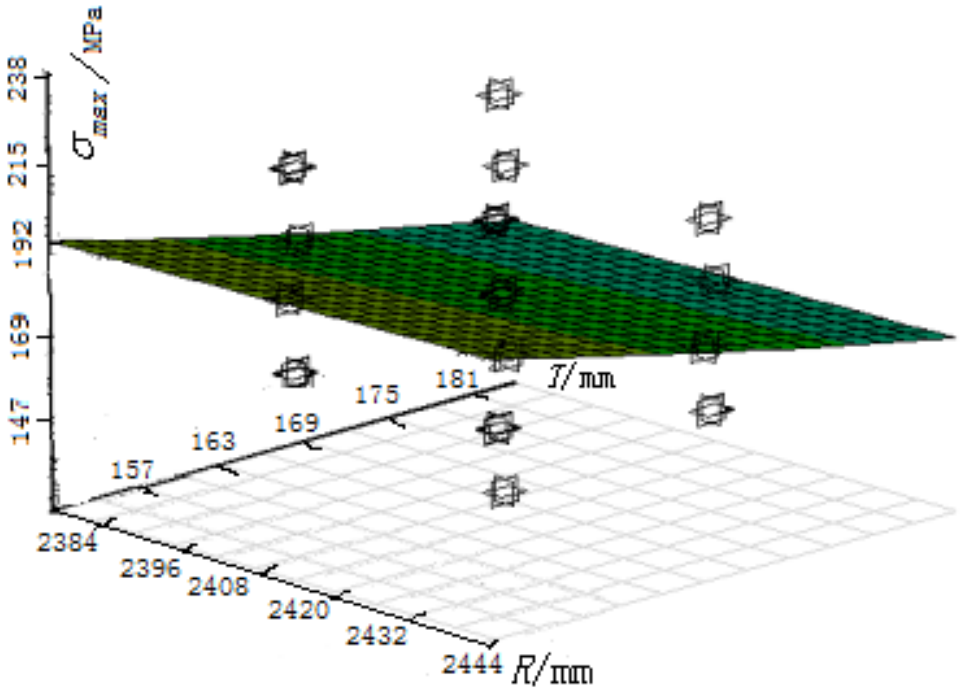

Fig. 4 Sampling Response surface

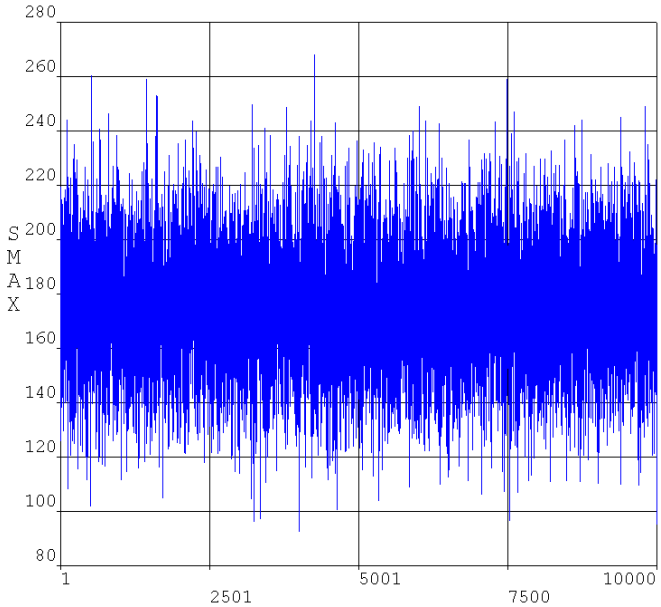

Fig. 5 Monte Carlo extending results

Table 1

Reliability analysis parameters for special large head

Mean value and standard deviation	Elastic modulus E/GPa	Poisson's ratio U	Inner radius R/mm	Wall thickness T/mm	Internal pressure P/MPa
Mean value	200	0.3	2415.5	168	20
Standard deviation	10	0.03	10	6	2.5

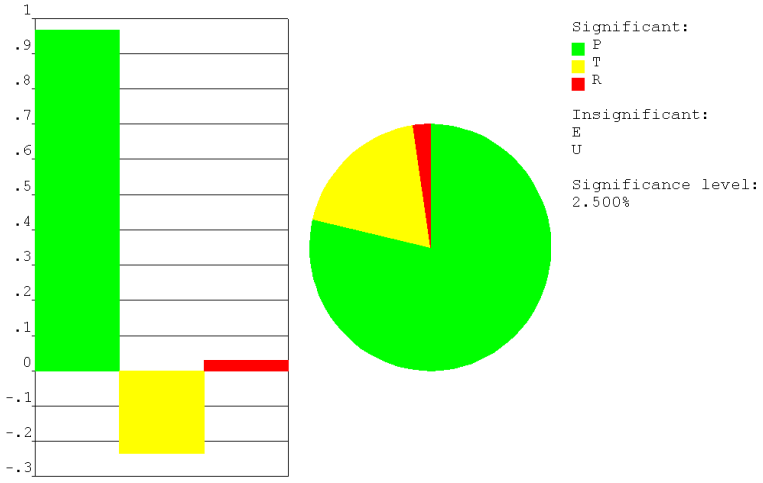

Fig. 6 Sensitivity analysis results

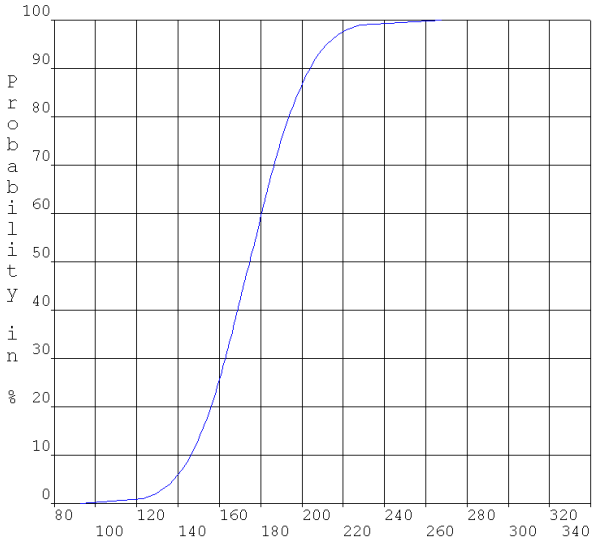

Fig. 7 Accumulative function distribution

The analysis results of high-pressure vessel using the response surface method based on Monte Carlo method are shown in Fig. 4. From Fig. 4, the maximum equivalent stress decreases as the wall thickness increases and increases as the internal pressure increases. The Monte Carlo expansion results are shown in Fig. 5. From Fig. 5, the maximum equivalent stress varies from 92.663 MPa to 268.05 MPa. The sensitivity analysis results are shown in Fig. 6. From Fig. 6, it's the maximum equivalent stress is greatly affected by the wall thickness, internal pressure and the radius of the spherical part, and is not sensitive to the material parameters. The cumulative calculation results are shown in Fig. 7. From Fig. 7, when each parameter fluctuates randomly in the range shown in Table 1, 95% of the maximum equivalent stress is less than 210 MPa, which is lower than the maximum allowable equivalent stress of 420 MPa of the container material. This further demonstrates the reliability of the container. Comparing the theoretical calculation formula with engineering practice, it can be seen that the sensitivity analysis results and parameters have a correct impact on the maximum equivalent stress of high-pressure vessels.

Fig. 8 The ultra-high pressure water tower

The high-pressure vessel installed in the water tower is shown in Fig. 8 and it has been responsible for high-pressure water storage for a long time. According to the monitoring results, it has been running well and its service life can meet the predicted design requirements. Due to the avoidance of manufacturing defects in the manufacturing process of this large pressure vessel, the maximum stress is the main cause of failure. Comparing the theoretical models, the maximum stress result calculated by finite element method is accurate. Therefore, the reliability of the pressure vessel is measured by the reliability of the maximum stress. The monitoring of pressure vessels in actual water towers shows that the design scheme based on this reliability analysis is reliable. This further demonstrates the accuracy of the theoretical and simulation results, laying a theoretical, simulation, and practical foundation for the optimization of the next generation of water tower high-pressure vessels.

4. Conclusion

The impact of randomness in geometric parameters, material parameters and loading parameters on the reliability of the ultra-high pressure vessels in water towers is studied. Based on the improvement in the design of the overall structure, the theoretical model of the variance of the maximum stress is established. The conclusions are drawn as follows:

(1) Based on probability theory, a theoretical model for the variance of maximum stress and reliability was established, and this model was used to calculate the typical ultra-high pressure vessel of the water tower;

(2) The finite element model was established. From the results of the finite element analysis, the maximum equivalent stress is located inside the head, at 174.794 Mpa;

(3) Based on the perturbation finite element method, the randomness of geometric parameters, material parameters and loading parameters was analyzed. The analysis results show that it works well and is consistent with its actual monitoring results.

The study is important to fine performance prediction and design for ultra-high pressure vessels.

Acknowledgement

This work was financially supported by the Key Research and Development Projects of Henan Province (182102310696).

R E F E R E N C E S

[1] *Yildirim, A., Yarimpabuc, D., Arikan, V., Eker, M., & Celebi, K.* "Nonlinear thermal stress analysis of functionally graded spherical pressure vessels", International Journal of Pressure Vessels and Piping, **vol. 200**, 2022, pp. 104830. https://doi.org/10.1016/j.ijpvp.2022.104830

[2] *Zhu, X. K., Wiersma, B., Johnson, W. R., & Sindelar, R.* "Burst pressure solutions of thin and thick-walled cylindrical vessels", Journal of Pressure Vessel Technology, **vol. 145**, no. 4, 2023, pp. 041303. https://doi.org/10.1115/1.4062334

[3] *Jármai, K., Sebe, I., & Szepesi, G.* "Fire safety design of pressure vessels", Engineering Review, **vol. 42**, no. 2, 2022, pp. 13-25. https://doi.org/10.30765/er.1615

[4] *Do V.D.,, Le Grognec, P.,, & Rohart, P.* "Closed-form solutions for the elastic–plastic buckling design of shell structures under external pressure", European Journal of Mechanics - A/Solids, **vol. 98**, 2022, pp. 104861. https://doi.org/10.1016/j.euromechsol.2022.104861

[5] *Oromiehie, E.,, Nagulapally, P.,, Donough, M.J.,, & Prusty, B.G.* "Automated manufacture and experimentation of composite overwrapped pressure vessel with embedded optical sensor", International Journal of Hydrogen Energy, **vol. 79**, no. 8, 2024, pp. 1215-1226. https://doi.org/10.1016/j.ijhydene.2024.06.364

[6] *Park, G.,, & Kim, C.* "Composite layer design using classical laminate theory for high pressure hydrogen vessel (Type 4)", International Journal of Precision Engineering and Manufacturing, **vol. 24**, no. 4, 2023, pp. 571-583. https://doi.org/10.1007/s12541-022-00752-w

[7] *Agag Jr, & G. M.* "Weld-joint design to optimize groove weld depth and mechanical properties for welding of nozzle onto pressure vessel", Welding International, **vol. 38**, no. 8, 2024, pp. 511-530. https://doi.org/10.1080/09507116.2024.2374727

[8] *Nguyen, T.T.,, Park, J.,, Bae, K.O.,, & Baek, U.B.* "Hydrogen-related degradation of fracture properties and altered fracture behavior of Cr–Mo steel used in hydrogen stationary vessels", International Journal of Hydrogen Energy, **vol. 53**, no. 1, 2024, pp. 1009-1024. https://doi.org/10.1016/j.ijhydene.2023.11.327

[9] *Ranjan, R.,, & Meena, A.* "Effect of martensite-austenite island decomposition during two-step tempering on the fracture surface morphology of impact and tensile tested Mn-Ni-Mo steel", Engineering Failure Analysis, **vol. 161**, 2024, pp.108325. https://doi.org/10.1016/j.engfailanal.2024.108325

[10] *Sowiński, K.* "Experimental and numerical verification of stress distribution in additive manufactured cylindrical pressure vessel - A continuation of the dished end optimization study", Thin-Walled Structures, **vol. 183**, no. 2, 2023, pp. 110336. https://doi.org/10.1016/j.tws.2022.110336

[11] *Yadav, M., Apte, C., Yelve, N. P., Gries, T., & Tewari, A.* "Exploring stress and deformation in filament-wound composite pressure vessel liners using PyMAPDL", International Journal of Hydrogen Energy, **vol. 71**, no. 6, 2024, pp. 493-505. https://doi.org/10.1016/j.ijhydene.2024.05.290

[12] *Bouhala, L., Koutsawa, Y., Karatrantos, A., & Bayreuther, C.* "Design of Type-IV Composite Pressure Vessel Based on Comparative Analysis of Numerical Methods for Modeling Type-III Vessels", Journal of Composites Science, **vol. 8**, no. 2, 2024, pp. 40. https://doi.org/10.3390/jcs8020040

[13] *Avcu, A., Seyedzavvar, M., Boğa, C., & Choupani, N.* "Characterizing the effects of liner and fiber-reinforced resin composite shell on fracture energy in type-III high-pressure composite tanks", Journal of the Brazilian Society of Mechanical Sciences and Engineering, **vol. 46**, no. 1, 2024, pp. 13. https://doi.org/10.1007/s40430-023-04598-9

[14] *Park, Y., Choi, J. H., Choi, J. B., & Kim, M. K.* "A stress intensity predictive model for reactor pressure vessel via coupled signal processing and machine learning model", Journal of Mechanical Science and Technology, **vol. 37**, no. 6, 2023, pp. 2881-2890. https://doi.org/10.1007/s12206-023-0514-6

[15] *Castiglione, T., Nicoletti, F., Ferraro, V., & Sangineto, C. M.* "CFD analysis of Part-Load operation of an Open-Circuit Induced-Draft cooling tower", Applied Thermal Engineering, **vol. 229**, 2023, pp. 120636. https://doi.org/10.1016/j.applthermaleng.2023.120636

[16] *Hadidi, A.* "Designing an energy storage system based on water tower pumping to store the energy generated by the turbo-expander implemented in a gas pressure reduction station", Journal of Energy Storage, **vol. 86**, no. Part A, 2024, pp. 111212. https://doi.org/10.1016/j.est.2024.111212